Optical and structural properties of β-$FeSi_2$ precipitate layers in silicon

B. Schuller[a)]
ZAM, Forschungszentrum Jülich, D-52425 Jülich, Germany

R. Carius
IPV, Forschungszentrum Jülich, D-52425 Jülich, Germany

S. Mantl
ISG-1/IT, Forschungszentrum Jülich, D-52425 Jülich, Germany

(Received 30 January 2003; accepted 31 March 2003)

Semiconducting iron disilicide (β-$FeSi_2$) precipitates in silicon were fabricated by ion beam synthesis. The samples were characterized by Raman spectroscopy, transmission electron microscopy, and photoluminescence spectroscopy. By comparison with a β-$FeSi_2$ single crystal, the silicide precipitates are found to be unstrained in all cases, so there is no correlation between strain and photoluminescence efficiency. Our results indicate that carrier recombination at silicon dislocations is sufficient to explain the photoluminescence in our samples. © *2003 American Institute of Physics.* [DOI: 10.1063/1.1576902]

INTRODUCTION

Semiconducting iron disilicide (β-$FeSi_2$) is considered as a promising material for silicon based optoelectronics due to its band gap of about 0.8 eV.[1,2] This energy corresponds to a wavelength of 1.55 μm, which is of considerable interest for applications in optical fiber based telecommunications.

In recent years, research interest has been focused on iron disilicide precipitates in a silicon host matrix. Notably, room temperature electroluminescence from a diode based on such a structure has been demonstrated.[3] This device has been fabricated by ion beam synthesis (IBS) (for a review of this method, see Ref. 4), producing silicide precipitates in the junction region of a conventional silicon *p-n* diode. Similar results have been reported for spherical iron disilicide precipitates grown by reactive deposition epitaxy.[5]

However, it is still a matter of debate whether the light emission in such a structure is really due to recombination in the silicide. There are two issues. First, in the spectral region where the band to band recombination from the silicide is expected, there are also lines originating from recombination at extended defects in the silicon matrix.[6] These so called *D* lines have also been used in a demonstrator light emitting device operating at room temperature.[7] Second, no light emission has been reported for β-$FeSi_2$ single crystals, supposedly because they lack sufficient purity. In addition, reports of light emission from epitaxial β-$FeSi_2$ layers on silicon have been quite scarce.[8,9] Thus, the intrinsic luminescence properties of beta iron disilicide are not well established.

Since it is difficult, using continuous wave photoluminescence (PL) measurements alone, to distinguish silicide related luminescence from dislocation related luminescence, additional information is needed. This can be gained by time dependent luminescence measurements. A direct, allowed transition is characterized by a short radiative lifetime[10] and, provided the defect density is low enough, a high quantum efficiency. However, quantum efficiency is difficult to measure directly. So far, only rough estimates of the quantum efficiencies achieved in β-$FeSi_2$ precipitate layers in silicon have been given, being on the order of 10^{-4} at low temperatures.[3] Consequently, information on the decay time of the light emission from the silicide layers would be very useful for resolving the issues mentioned. An earlier report on the decay time of the 1.55 μm emission line gave a long decay time of 60 μs at a temperature of 20 K, which the authors interpreted as indicating an indirect transition.[11]

It has been shown experimentally and theoretically that iron disilicide is an indirect semiconductor[12–15] with a direct gap some tens of meV above the indirect one. The calculations have clearly shown a high sensitivity of the β-$FeSi_2$ band structure to strain. In some epitaxial configurations, β-$FeSi_2$ on a silicon substrate is predicted to have a direct band gap. Whether these strain effects have any influence on the optical properties of iron disilicide precipitates in silicon has not yet been shown conclusively, although some steps in this direction have been taken.[16,17]

In this work, we focus on experimental attempts to clarify the physical origin of the 0.8 eV light emission from β-$FeSi_2$ precipitate layers in silicon. The precipitate microstructure has been varied by modifying the processing parameters such as implant dose and annealing scheme. The structural quality and the strain state of the silicide were investigated by Raman spectroscopy. Continuous wave and time resolved photoluminescence spectroscopy were used to investigate the optical properties of the layers.

EXPERIMENT

As starting material we used high resisitivity, *n*-type, float zone (100) silicon wafers. Iron (^{56}Fe) was implanted at an energy of 200 keV. The projected range of this implant is 150 nm.

a)FAX: (+49)2461 61 6656; electronic mail: b.schuller@fz-juelich.de

TABLE I. Sample processing details. The implantation energy was 200 keV in all cases.

Sample	Iron dose	Furnace annealing	Rapid thermal annealing
A	3×10^{17} /cm^2	830 °C/18 h	—
B	3×10^{17} /cm^2	900 °C/18 h	—
C	3×10^{17} /cm^2	830 °C/18 h	900 °C/10 min
D	1×10^{16} /cm^2	830 °C/18 h	—
E	2×10^{16} /cm^2	830 °C/18 h	900 °C/9 min+1100 °C/5 s
F	2×10^{16} /cm^2	830 °C/18 h	900 °C/9 min+1100 °C/30 s

During the implantation the wafer was heated to 450 °C to prevent amorphization of the silicon. The samples were annealed in a conventional furnace at 830–900 °C for 18 h in vacuum. Prior to the anneal, the samples were capped with 50 nm SiO_2 deposited by plasma enhanced chemical vapor deposition at 350 °C to protect the samples from contamination and thermal etching.

In some cases, rapid thermal annealing in an argon atmosphere was performed prior to the furnace annealing.

We distinguish ''high dose'' samples, where an iron dose of 3×10^{17} cm^{-2} was implanted, and ''low dose'' samples, where the dose was 1 or 2×10^{16} cm^{-2}. Table I gives an overview about the processing parameters for the samples investigated in this work. A β-$FeSi_2$ single crystal grown by the chemical transport method was provided to us by L. Ivanenko.[18]

Raman spectra were recorded at room temperature by a liquid nitrogen cooled multichannel charge-coupled device (CCD) detector attached to a SPEX 1404 double monochromator. The resolution of the Raman measurements is limited by the discrete channels of the CCD, and is about 0.5 cm^{-1}. As excitation source the 647 nm line of a krypton ion laser was used.

We used two different setups to measure continuous wave (cw) PL and time resolved PL, respectively. The cw spectra were measured in a Bruker IFS66v Fourier transform spectrometer, using a liquid nitrogen cooled germanium detector. Excitation was provided by the 488 nm line of an argon ion laser, with an excitation flux of 10 mW/mm^2. The illuminated area on the sample was about 20 mm^2. Time resolved photoluminescence was measured using a time correlated photon counting setup connected to a SPEX 1681 single monochromator. A Hamamatsu R5509-72 photomultiplier tube (PMT) served as a detector; its spectral sensitivity range is 300–1700 nm. The PMT is operated at a temperature of −80 °C to reduce the dark current to less than 1 count per microsecond. As excitation source we used a 504 nm dye laser, which is pumped by a nitrogen laser operating at 337 nm. The laser provides 5 ns wide pulses at a frequency of 10 Hz. The average output power is 100 μJ per pulse, which was focused to a 1 mm^2 spot on the sample. In pure silicon, the penetration depth of the 504 nm light is about 1 μm. In iron disilicide, with its much higher absorption, the penetration depth is approximately 30 nm.

The setup can be operated in two modes: (i) the time decay of the luminescence at a given wavelength can be measured; (ii) spectra can be measured within a fixed time window with respect to the excitation pulse. This second mode allows taking ''snapshots'' of the PL spectrum, thus making it possible to look for ''fast'' and ''slow'' components of the luminescence, i.e., to check whether the luminescence spectrum changes with time.

RESULTS AND DISCUSSION

The microstructure of the ''high dose'' samples produced by implantation of 3×10^{17} cm^{-2} Fe^+ and annealing using various schemes (see Table I) is shown in the cross sectional transmission electron microscopy (TEM) micrographs in Fig. 1. In the case of a single furnace annealing step at 830 °C, large, irregular silicide precipitates are formed (Fig. 1, top). Annealing at 900 °C leads to a much worse microstructure (Fig. 1 middle). The structure of the silicide layer is greatly improved by the additional rapid thermal annealing step performed in the case of sample C. As the cross sectional TEM micrograph in Fig. 1 (bottom) shows, a 180–200 nm thick layer with a very flat interface to the silicon substrate is formed. However, the silicide layer is not completely continuous.

The crystalline quality of the individual grains of all three of the high dose samples (A, B, and C) is very good. This is evidenced by the Raman spectra shown in Fig. 2. The characteristic β-$FeSi_2$ lines[19] are very narrow. The full width at half maximum of the 246 cm^{-1} main peak is 2.5 cm^{-1}; this is comparable to the values found in the literature for bulk β-$FeSi_2$ crystals. For comparison, the topmost graph in Fig. 2 shows a Raman spectrum of a β-$FeSi_2$ single crystal measured with our system. The additional weak peak at ~300 cm^{-1} present in the β-$FeSi_2$/Si samples is attributed to the LA phonon of the silicon matrix. It is important to note that the positions of the β-$FeSi_2$ peaks agree to within 0.5 cm^{-1} in all samples, including the single crystal.

The presence of strain would manifest itself in a Raman line shift, or, in the case of a distribution of precipitates in different strain states, a broadening of the lines. So we conclude that the β-$FeSi_2$ has fully relaxed during the 18 h annealing procedure. The continuous wave photoluminescence at low temperature (10 K) of the high dose samples (A, B, and C) is shown in Fig. 3. All samples show PL of similar intensity, with a broad feature at 0.8 eV. Additionally, in the case of samples A and B the silicon exiton peak at 1.097 eV can be observed. In the structurally better sample C, the overall PL intensity of the 0.8 eV peak is similar. The silicon exciton peak cannot be observed in this case, since the silicide layer is almost continuous, preventing excitation of the silicon substrate. The luminescence decreases drastically upon temperature increase (not shown), indicating a strong influence of nonradiative processes. The PL intensity of the

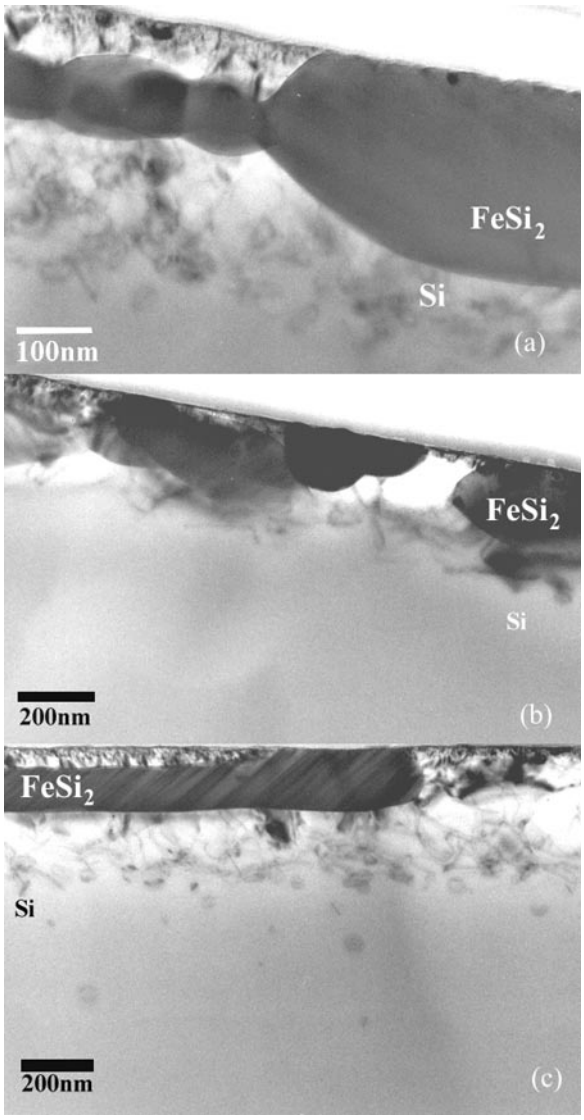

FIG. 1. Cross section TEM micrographs of high dose β-$FeSi_2$/Si samples A (top), B (middle), and C (bottom). For the processing details, see Table I.

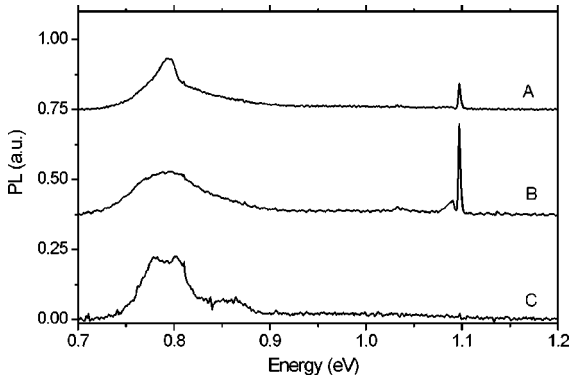

FIG. 3. Photoluminescence spectra of β-$FeSi_2$/Si samples A, B, and C taken at 10 K.

high dose samples is too low to perform time resolved measurements. Consequently, an identification of the physical recombination mechanism is impossible. However, in view of the low efficiency of the light emission, a direct transition in the silicide is highly unlikely.

We now turn to the structural and optical properties of the low dose samples. A cross-sectional TEM micrograph of the precipitate layer formed after implantation of 10^{16} Fe/cm^2 and annealing at 830 °C for 18 h (sample D) is shown in Fig. 4. The silicide precipitates are located at a depth of about 180 nm and are mostly faceted and aligned along {111} planes. They are of excellent crystalline quality, as evidenced by the Raman spectrum shown in Fig. 5. Again, we find very narrow Raman lines at positions coinciding with those of the reference sample C and the β-$FeSi_2$ single crystal. The additional broad peak at 300 cm^{-1} that is not seen in the single crystal and that is only weakly present in the high dose samples originates from the silicon substrate (the LA phonon). Again, we conclude from the positions and the widths of the Raman peaks that the silicide precipitates are fully relaxed.

The continuous wave PL spectrum at $T=6$ K of this sample (D) is shown in Fig. 6 (inset). The main peak at 0.8 eV is accompanied by weaker peaks at 0.87 and 0.93 eV, and a broad background component. The peak locations coincide with those of the well known *D* lines originating from dislocations in the silicon matrix.[6] However, the "*D*4" line at ~1

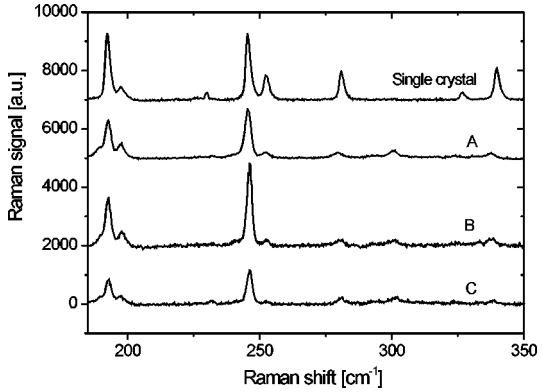

FIG. 2. Raman spectra of β-$FeSi_2$/Si samples A, B, and C. For comparison, a spectrum taken on a β-$FeSi_2$ single crystal is shown. The spectra have been vertically shifted for clarity.

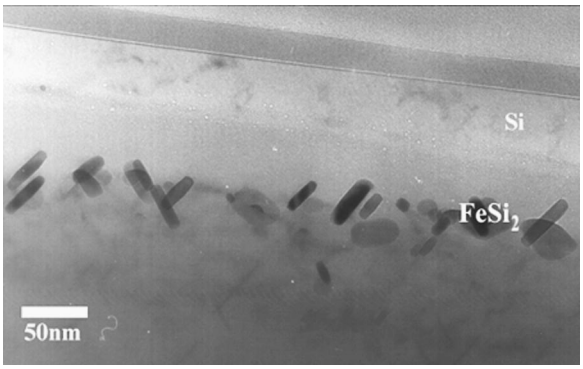

FIG. 4. Cross section TEM of β-$FeSi_2$ precipitates in Si (sample D), produced by hot implantation of 1×10^{16} Fe cm^{-1} and annealing at 830 °C for 18 h.

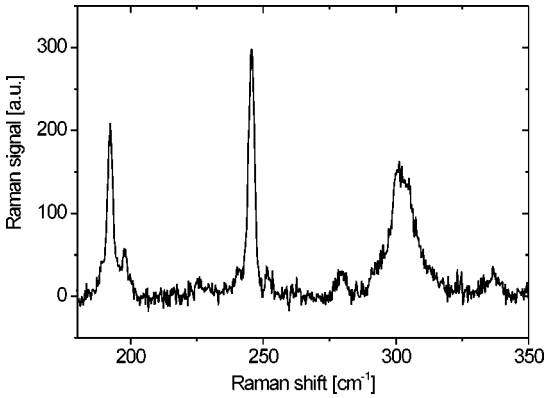

FIG. 5. Raman spectrum of β-$FeSi_2$ precipitates in Si (sample D).

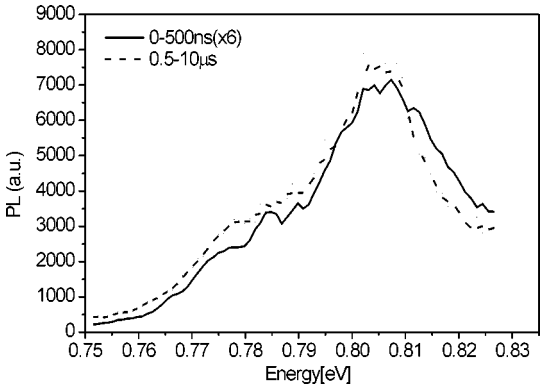

FIG. 7. PL spectra of β-$FeSi_2$/Si sample D at 10 K taken at different time windows 0–500 ns and 0.5–10 μs with respect to the excitation. The spectra have been normalized to the same peak intensity.

eV is not present in our samples. The overall PL intensity is two orders of magnitude higher than in the high dose samples. We find that the dependence of the PL intensity I on the excitation power P is given approximately by a square root law $I \sim P^{0.5}$ with a tendency to saturate at high excitation. This was already noted for IBS β-$FeSi_2$ by Katsumata and co-workers.[20] Similar behavior is reported for the D line dislocation luminescence in silicon based samples.[21] The time dependence of the 0.8 eV emission at $T=10$ K is given in Fig. 6. The decay curve can be fitted well by two exponentials, with a ''fast'' component having a decay time of 4 μs, and a ''slow'' component which has a decay time of 17 μs. A similar behavior has been reported by Fukatsu *et al.* for dislocation PL in SiGe/Si layers,[21] where the decay times were ~200 and 1000 ns. The decay times in our samples decrease with increasing temperature, which can be explained by an increased influence of nonradiative recombination.

The spectral features of the 0.8 eV emission do not change significantly during the time decay, as shown in Fig. 7, where we show two spectra taken at time windows of 0–500 ns and 0.5–10 μs, respectively.

The position and the width of the 0.8 eV peak change only marginally, if at all, on varying the time window. The results of the time resolved measurements rule out the possibility of a superposition of silicide related luminescence and D line luminescence, since one would expect the former to have a different line shape compared to the latter. To summarize the results of the PL measurements, we found no evidence for a fast, direct transition. The observed behavior is consistent with the assumption of an indirect transition. In fact, it is entirely possible and even sensible to attribute the observed PL properties to recombination at silicon defects, since only a single luminescence mechanism is found to be present.

Finally, we present a comparison of luminescence from a $FeSi_2$ precipitate layer where no semiconducting (β-phase) silicide is present, with that from a β-$FeSi_2$ sample prepared using comparable conditions. Figure 8 shows the PL spectra for samples E and F, which underwent a high temperature (1100 °C) annealing step prior to the 830 °C/18 h furnace anneal. For sample F, annealing for 30 s above the β to α phase transition temperature results in a complete loss of the β-phase Raman signature (Fig. 8, inset), i.e., only the α phase is present. The PL signal, however, is still present, albeit with its intensity reduced to about 50%. Therefore, it is reasonable to assume that the PL in the β-$FeSi_2$ sample E does not originate from the silicide, but from defects in the silicon host material.

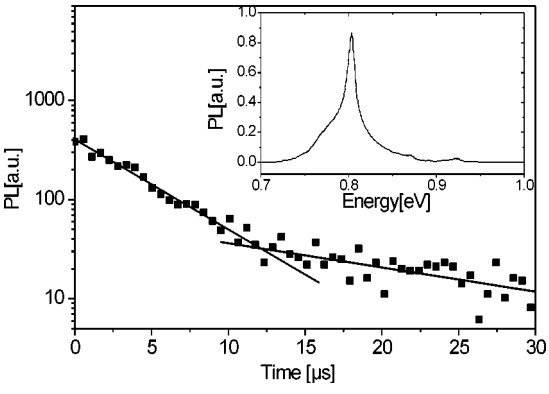

FIG. 6. Time dependent photoluminescence of β-$FeSi_2$/Si sample D, taken at $T=10$ K and a wavelength of 1545 nm. Inset: continuous wave PL taken at $T=6$ K.

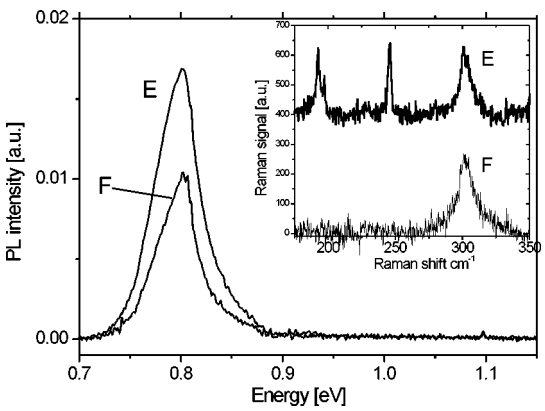

FIG. 8. Continuous wave PL spectra at $T=10$ K of $FeSi_2$/Si samples E and F. The inset shows the corresponding Raman spectra.

SUMMARY AND OUTLOOK

We have presented optical and structural investigations of β-$FeSi_2$/Si layers, where the silicide microstructure was varied from small precipitates to a nearly continuous layer.

Raman spectroscopy shows that the silicide is crystalline and fully relaxed in all samples. Consequently, there is no correlation of strain with the variation over two orders of magnitude in photoluminescence efficiency. The photoluminescence properties of our samples, such as decay time, excitation power, and temperature dependence, are very similar to those of dislocation related luminescence from damaged silicon. No contribution to the luminescence that could be attributed solely to recombination in the silicide could be singled out. However, the fact that the luminescence in our samples can be solely attributed to silicon defects is not a general conclusion. Other authors[22,23] have taken great care to make sure that certain types of precipitates embedded in defect-free silicon do indeed contribute to the observed photoluminescence. Their findings gave no indication for a direct transition. To achieve a defect-free silicon matrix using ion beam synthesis is very difficult, however. It may be necessary to use a different synthesis method, for example, reactive deposition epitaxy.[5]

These results show that the suitability of iron disilicide precipitate layers for optical emitters is at least controversial. Since the intrinsic luminescence properties of iron disilicide are still unknown, disentangling silicide related luminescence from defect luminescence in these heterosystems is very difficult.

ACKNOWLEDGMENTS

We would like to thank St. Lenk for the TEM micrographs, L. Ivanenko for the β-$FeSi_2$ single crystals, M. Gebauer for performing the ion implantations, and M. Hülsbeck for technical assistance. Part of this work was funded by the EU under Project No. 28740 (SiLITE).

[1] M. C. Bost and J. E. Mahan, J. Appl. Phys. **74**, 1138 (1993).
[2] For a recent review, see *Semiconducting Silicides*, edited by V. E. Borisenko (Springer, Berlin, 2000).
[3] D. Leong, M. Harry, K. J. Reeson, and K. P. Homewood, Nature (London) **387**, 686 (1997).
[4] S. Mantl, Mater. Sci. Rep. **8**, 1 (1992).
[5] T. Suemasu, Y. Negishi, K. Takahara, and F. Hasegawa, Jpn. J. Appl. Phys., Part 2 **39**, L1013 (2000).
[6] R. Sauer, J. Weber, J. Stolz, E. R. Weber, K.-H. Küsters, and H. Alexander, Appl. Phys. A: Solids Surf. **36**, 1 (1985).
[7] E. Sveinbjörnsson and J. Weber, Appl. Phys. Lett. **69**, 2686 (1996).
[8] C. A. Dimitriadis, J. H. Werner, S. Logothedis, M. Stutzmann, J. Weber, and R. Nesper, J. Appl. Phys. **68**, 1726 (1990).
[9] S. Chu, T. Hirohada, and H. Kan, Jpn. J. Appl. Phys., Part 2 **41**, L299 (2002).
[10] J. Pankove, *Optical Processes in Semiconductors* (Dover, New York, 1972).
[11] C. Spinella, S. Coffa, C. Bongiorno, S. Pannitteri, and M. G. Grimaldi, Appl. Phys. Lett. **76**, 73 (2000).
[12] K. Radermacher, R. Carius, and S. Mantl, Nucl. Instrum. Methods Phys. Res. B **84**, 163 (1994).
[13] A. B. Filonov *et al.*, J. Appl. Phys. **79**, 7708 (1996).
[14] D. Migas and L. Miglio, Phys. Rev. B **62**, 11 063 (2000).
[15] K. Yamaguchi and K. Mizushima, Phys. Rev. Lett. **86**, 6006 (2001).
[16] A. G. Birdwell, R. Glosser, D. N. Leong, and K. P. Homewood, J. Appl. Phys. **89**, 965 (2001).
[17] B. Schuller, R. Carius, and S. Mantl, Microelectron. Eng. **55**, 219 (2001).
[18] G. Behr, L. Ivanenko, H. Hinzelberg, and A. Heinrich, Thin Solid Films **381**, 276 (2001).
[19] K. Lefki and P. Muret, Appl. Surf. Sci. **65/66**, 772 (1993).
[20] H. Katsumata *et al.*, J. Appl. Phys. **80**, 5955 (1996).
[21] S. Fukatsu, Y. Mera, M. Inoue, K. Maeda, H. Akiyama, and H. Sakakai, Appl. Phys. Lett. **68**, 1889 (1996).
[22] M. G. Grimaldi, C. Bongiorno, C. Spinella, E. Grilli, L. Martinelli, M. Gemelli, D. B. Migas, L. Miglio, and M. Fanciulli, Phys. Rev. B **66**, 085319 (2002).
[23] L. Martinelli, E. Grilli, D. B. Migas, L. Miglio, F. Marabelli, C. Soci, M. Geddo, M. G. Grimaldi, and C. Spinella, Phys. Rev. B **66**, 085320 (2002).